Kinetics of Adsorption-Induced Deformation of Microporous Carbons

Andrei L. Kolesnikov,[*,†] Andrey V. Shkolin,[‡] Ilya E. Men'shchikov,[‡] and Gennady Y. Gor[*,†,¶]

†*Otto H. York Department of Chemical and Materials Engineering, New Jersey Institute of Technology, Newark, New Jersey 07102, United States*

‡*Frumkin Institute of Physical Chemistry and Electrochemistry of Russian Academy of Science (IPCE RAS), Moscow 119071, Russian Federation*

¶*Department of Mechanical and Aerospace Engineering, Princeton University, Princeton, New Jersey 08544, United States*

E-mail: kolesnik@njit.edu; gor@njit.edu

Abstract

Equilibrium and kinetic behavior of adsorption-induced deformation attracted a lot of attention in the last decades. The theoretical and experimental works cover activated carbons, coals, zeolites, glasses, etc. However, most of the theoretical works describe only the equilibrium part of the deformation process or focus on the time evolution of the adsorption process. The present paper aims to cover the existing gap, using the thermodynamic framework combined with the diffusion-based description of adsorbate time evolution inside an adsorbent. We obtained self-consistent equations describing equilibrium and out-of-equilibrium adsorption as well as deformation processes. Further, the obtained equations were verified on the experimental data of carbon dioxide and methane on activated carbons. The model is capable of describing both equilibrium and kinetic adsorption and adsorption-induced deformation data. Additionally,

we studied the possible influence of slow relaxation processes in the adsorbent on the adsorption process. The current work helps to interpret experimental data on time-dependent adsorption-induced deformation.

Introduction

Sorption-induced deformation is a ubiquitous phenomenon and can be defined as a response of the adsorbent to an increase of an adsorbate amount inside.[1–3] Generally, one does not necessarily need to distinguish between adsorption and absorption: both processes lead to dimensional changes in a host material. However, the underlying mechanisms and, in most cases, observable macroscopic changes will be different. The magnitude of adsorption-induced deformation (AID) covers the range from fraction of a percent up to several percent.[1] While, polymer strain due to solvent absorption, which is typical e.g. for water on bio-polymers, reaches tens of percent.[4–6] The differences also appear in both thermodynamic and kinetic descriptions of adsorption-induced deformation. Due to the small strain magnitudes, it is often assumed that the adsorption and deformation can be decoupled. On contrary, in polymeric systems swelling and absorption is coupled and that have to be taken into account in theoretical models[7–10] and molecular simulations.[11–13] In this work, we focus on the theoretical description of adsorption-induced deformation kinetics of microporous activated carbons (ACs), which are important industrial adsorbents.

Separately thermodynamics of AID[14–19] and sorption kinetics[20–23] into inert host were theoretically and experimentally studied for various types of microporous solid materials, including activated carbons. The latter provides information about their transport properties which is significant since many industrial and natural processes occur far from thermodynamic equilibrium. Measurements of equilibrium adsorption-induced deformation are inseparably linked to its kinetics via an equilibration process. In addition, AID kinetics contains information about not only the transport properties of the adsorbate (e.g. diffusivity) but also about the material elasticity. Thus, it presents a valuable experimentally measurable

quantity. However, to the best of our knowledge, the kinetics of AID in activated carbons has not been studied in depth theoretically and experimentally. Thus, the main goal of the paper is to propose a model describing adsorption and AID kinetics consistently with previously developed approaches. Namely, a thermodynamic approach developed for AID[24–26] and a diffusion-based approach for the description of adsorption kinetics.[20,27]

In detail, adsorption-induced deformation kinetics has not been studied theoretically except for coal.[28–30] Even much simpler systems, that demonstrate AID, such as microporous carbons were studied less extensively. In Ref.,[31] Perrier et al presented an experimental setup based on the manometric adsorption measurements and digital image correlation (DIC) techniques. It allows the authors[31] to measure adsorption and deformation simultaneously. They studied the equilibrium and kinetic deformation of activated carbon during CO_2 and CH_4 sorption. In Ref.[29] the authors investigated CO_2 adsorption/AID behavior of coal matrix, i.e. cleates-free samples were collected to conduct experiments. The CO_2 diffusion and AID measurements were performed and further used to verify the proposed numerical model. However, the influence of the shape of strain isotherm on the kinetics of AID was not studied. It can have a crucial effect due to the possible minimum at low adsorbate pressure. The latter was observed in many microporous materials, for example, activated carbons and zeolites.[1,15,18,32]

In this work, we proposed a thermodynamic-based approach for the description of equilibrium and kinetics of adsorption and adsorption-induced deformation. We used radial displacement and adsorbate concentration as order parameters in our system. Since, they can be easily correlated with measurable quantities we, first of all, verified our model by comparing its results with experimental data. The model was applied to two data sets, namely carbon dioxide on AC *Chemviron* from Ref.[31] and methane on AC *T-3*,[33] measured by us. After the model had been validated, we predicted AID kinetics for two common shapes of strain isotherms - with and without minimum at low relative pressures. Additionally, we investigated the possible impact of slow material relaxation rates, i.e. having comparable

with adsorbate diffusion timescale, on the adsorption process. The current model can help in the interpretation of out-of-equilibrium AID experimental data.

Experimental section

The *T-3* adsorbent is manufactured from peat using chemical activation technology. After grinding and separating the raw material, it is impregnated with potassium sulfide K_2S and mixed until a homogeneous elastic paste is obtained. The paste is pressed and pelletized through dies. Obtained extruded pellets are dried in a rotary kiln and subjected to carbonization, where residual moisture and volatile substances are removed by flue gases, and the organic component of the peat is decomposed. The activation process of the resulting carbonized semi-product is carried out in a rotary kiln at temperatures 780-860 °C. During the process the final removal of volatile substances takes place, the material is enriched with carbon, its strength and density increase, and finally a porous structure is formed. The activated product is cooled and sent to the washing and drying stages. The final adsorbent form factor is cylindrical granules ($d = 2.3\,\mathrm{mm}$; $l = 5.1\,\mathrm{mm}$).

A custom-made induction-type dilatometer was employed to quantify the deformation of the linear carbon sample. The dilatometer was used as part of an experimental setup that included gas injection systems, a set of sensors to control the measurement, a vacuum station, and a gas pipeline system. The bench offers the possibility of measuring the linear deformation of porous granular materials in a wide range of pressures and temperatures, spanning from 1 Pa to 20 MPa and from 213 to 393 K, respectively.

In our studies, the adsorption-induced linear deformation of the adsorbent is a function of the changes in the readings of the inductive displacement sensor, which are dependent on pressure at a given temperature. In the calculations, the change in the linear dimensions of the adsorbent granules was taken into account, with the correction obtained from the experiments with a quartz mockup under identical thermodynamic conditions.

The uncertainty of the relative linear deformation measurement of the carbon sample was estimated in accordance with the ISO requirements.[34] In general, the measurement uncertainty of the relative linear deformation depends on the adsorbent in question, its properties, and the thermodynamic conditions under which the measurement is taken. In our experiments, the average measurement uncertainty was found to be uc(η)=2.0 % and the extended uncertainty was U(η) = 6.0 % at the 95% confidence level.

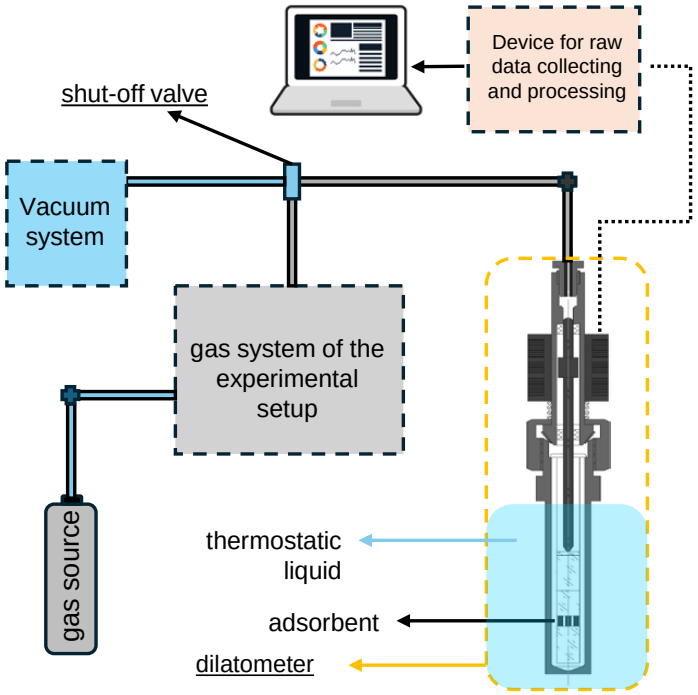

Figure 1: Sketch of the experimental setup used for measurements of adsorption-induced deformation.

The bench allows for the measurement of both equilibrium and kinetic characteristics of deformation. The procedure and conditions for measuring equilibrium deformation characteristics are described in detail in the paper.[35] In Fig. 1, we present a sketch of the experimental setup for kinetic measurements of AID. To measure the kinetic characteristics, a carbon sample was maintained at a pressure of 1 bar at a temperature of 293 K. The dilatometer was disconnected from the gas system of the experimental setup, in which the

operating pressure of the system was created corresponding to the final pressure of the kinetic experiment. In this instance, gas lines were connected to a gas source in order to ensure constant pressure within the stand. Subsequently, the shut-off valve was opened, allowing the supply of gas to the dilatometer to an operating pressure. Given that pressure equalization within the stand and the dilatometer was achieved in less than one second, the pressure increase was considered instantaneous, and the kinetic process was isobaric. The change in deformation of the carbon granule was recorded every second until equilibrium was established.

Model

Consider a spherical particle of microporous adsorbent (see Fig. 2) immersed in the adsorbate vapor at fixed temperature T and pressure P. Thus, the kinetic processes are caused by a sudden change of adsorbate pressure surrounding the adsorbent particle. These processes drive the system to a new thermodynamic equilibrium state corresponding to the applied gas pressure. We assume that physical adsorption takes place in the homogeneous solid phase, i.e. with uniform properties distribution (for example, unimodal pore size distribution, constant elastic moduli, isotropic deformation,[36] etc.). The model considers small strains, typical for gas adsorption in solid microporous adsorbents, such as activated carbons,[16,32] zeolites,[15,37,38] porous glasses,[39] etc. Thus, following the ideas of linear elastic theory[40] we don't consider the change of the coordinates, i.e. assuming that current and reference coordinate systems are the same.

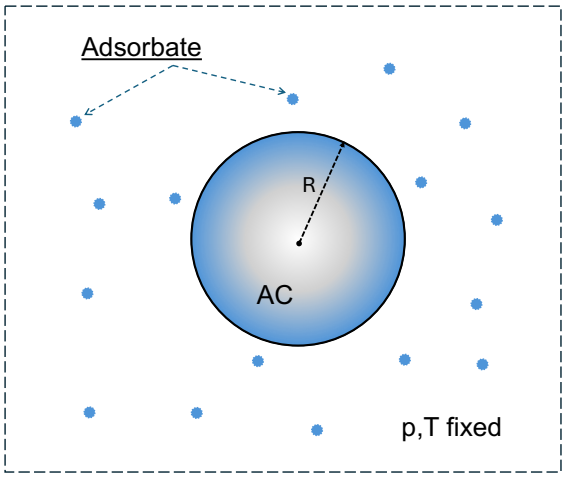

Figure 2: Schematic representation of the system under consideration. A microporous activated carbon particle is assumed to have a spherical shape with radius R. The adsorbate molecules in the bulk and adsorbed states are represented by blue dots and by blue gradient respectively (not to scale). We assume that the adsorption process takes place at constant T and p.

The osmotic potential (Ω) for the case of radial deformation can be written as a functional of radial displacement $u(r)$:

$$\Omega[u(r), \rho_{\mathrm{n}}(r)] = 4\pi \int_0^R \mathrm{d}r r^2 \Big\{ f_{\mathrm{s}}^0 + f_{\mathrm{el}}(u) + f_{\mathrm{ads}}(\varepsilon_{\mathrm{V}}, \rho_{\mathrm{n}}) - \rho_{\mathrm{n}}\mu_{\mathrm{b}} + (1+\varepsilon_{\mathrm{V}})p \Big\}, \tag{1}$$

$$f_{\mathrm{el}}(u) = \frac{1}{2}\left(K - \frac{2}{3}G\right)\left(\frac{\partial u}{\partial r} + \frac{2u}{r}\right)^2 + G\left[\left(\frac{\partial u}{\partial r}\right)^2 + 2\left(\frac{u}{r}\right)^2\right] \tag{2}$$

where f_{s}^0 and $f_{\mathrm{el}}(u)$ are the adsorbent reference and elastic part of Helmholtz free energy, respectively; K and G are the effective bulk and shear moduli of the porous medium; ε_{V} is the volumetric strain, i.e. trace of the strain tensor; μ_{b} is the adsorbate chemical potential in the vapor phase; ρ_{n} is the volumetric adsorbate density within the solid; p is the bulk pressure. We use lattice gas approximation for the density of adsorbate Helmholtz free

energy $f_{\mathrm{ads}}(\varepsilon_{\mathrm{V}}, \rho_{\mathrm{n}})$:[41]

$$f_{\mathrm{ads}}(\varepsilon_{\mathrm{V}}, \rho_{\mathrm{n}}) = k_{\mathrm{B}}T[-\rho_{\mathrm{m}}(\varepsilon_{\mathrm{V}})\ln(\rho_{\mathrm{m}}(\varepsilon_{\mathrm{V}})) + \rho_{\mathrm{n}}\ln(\rho_{\mathrm{n}}) + (\rho_{\mathrm{m}}(\varepsilon_{\mathrm{V}}) - \rho_{\mathrm{n}})\ln(\rho_{\mathrm{m}}(\varepsilon_{\mathrm{V}}) - \rho_{\mathrm{n}})] + \rho_{\mathrm{n}}\phi(\varepsilon_{\mathrm{V}}) \tag{3}$$

with $\rho_{\mathrm{m}}(\varepsilon_{\mathrm{V}})$ being maximum value of ρ_{n}, $\phi(\varepsilon_{\mathrm{V}})$ is the value of external potential and, k_{B} is the Boltzmann constant. The first part of Eq. 3 is the volumetric density of Helmholtz free energy of non-interacting adsorbate on the adsorbent surface. The second part describes an interaction of adsorbate with the adsorbent surface. Here, we considered that the maximum adsorbed amount and interaction energy may differ during the deformation process.[26] The bulk chemical potential and equation of state were also derived from the lattice gas approximation, assuming that number of molecules is much smaller than number of lattice cells:

$$\mu_{\mathrm{b}} = k_{\mathrm{B}}T\ln(p\sigma/k_{\mathrm{B}}T) \tag{4}$$

$$p = k_{\mathrm{B}}T\rho_{\mathrm{b}}, \tag{5}$$

here σ is the volume of the lattice cell, ρ_{b} is the density of gas molecules in the bulk. During adsorption process the adsorbent properties may change, here we consider linear variations of $\rho_{\mathrm{m}}(\varepsilon_{\mathrm{V}})$ and $\phi(\varepsilon_{\mathrm{V}})$:

$$\phi(\varepsilon_{\mathrm{V}}) = \phi_0 + \kappa\varepsilon_{\mathrm{V}} \tag{6}$$

$$\rho_{\mathrm{m}}(\varepsilon_{\mathrm{V}}) = \rho_{\mathrm{m},0} + \lambda\varepsilon_{\mathrm{V}}. \tag{7}$$

The linear approximation is valid only in the limit of small strains. Otherwise, it may lead to results which can be incorrect even qualitatively. The four newly introduced parameters represent the first two terms of Maclaurin series having the following meaning: $\rho_{\mathrm{m},0}$ and ϕ_0 are maximum adsorbate density and external potential in the reference state; κ and λ are the parameters defining the response of porous body on the adsorption process.

In the state of thermodynamic equilibrium Ω is minimal, thus we can obtain the system of equations defining equilibrium $(\varepsilon_{\mathrm{V}}, \rho_{\mathrm{n}})$ values (see SI for more details):

$$\rho_{\mathrm{n}}^{\mathrm{eq}} = \frac{\rho_{\mathrm{m},0} b p}{1 + bp}, \tag{8}$$

$$K\varepsilon_{\mathrm{V}}^{\mathrm{eq}} = -f'_{\mathrm{ads}}(\rho_{\mathrm{n}}^{\mathrm{eq}}) - p, \tag{9}$$

as well as the equation for adsorbent volumetric deformation during the diffusion process:

$$\varepsilon_{\mathrm{V}} = \frac{-3R^{-3}\int\limits_{0}^{R} \mathrm{d}r r^2 f'_{\mathrm{ads}}(\rho_{\mathrm{n}}) - p}{K}, \tag{10}$$

where $f'_{\mathrm{ads}}(\rho) = -k_{\mathrm{B}}T\lambda \ln[\rho_{\mathrm{m},0}/(\rho_{\mathrm{m},0} - \rho)] + \kappa\rho$. Due to our assumption of the small strain magnitude, we decouple deformation from adsorption in the final equations. It allows us to sequentially apply Eqs. 8 and 9 to experimental data for parameterizing the model.

In order to describe the adsorption kinetics we use the diffusion approximation[20,21] to formulate the mass conservation law for adsorbate molecules inside microporous body:

$$\frac{\partial \rho_{\mathrm{n}}}{\partial t} = \frac{1}{r^2}\frac{\partial}{\partial r}\left(r^2 M \rho_{\mathrm{n}} \frac{\partial \mu}{\partial r}\right), \tag{11}$$

where $\mu = k_{\mathrm{B}}T \ln(\rho_{\mathrm{n}}/\rho_{\mathrm{m}} - \rho_{\mathrm{n}}) + \phi$ is the local chemical potential of the fluid and M is the adsorbate mobility. In the context of mass transfer we use the following notation $\rho_{\mathrm{n}} = \rho_{\mathrm{n}}(r,t)$ for simplicity of the equations. Typically, for a porous solid material, the kinetics of deformation is much faster than the diffusion, thus we can use the same solution for the displacement field as in the equilibrium. However, in that case, $u(r)$ has also a time dependence through the ρ_{n}.

Here, we also can decouple the diffusion and deformation process, thus obtaining (see SI

for more details):

$$\frac{\partial \rho_{\mathrm{n}}}{\partial t} = \frac{1}{r^2}\frac{\partial}{\partial r}\left(r^2 D_0 \frac{\rho_{\mathrm{m},0}}{\rho_{\mathrm{m},0} - \rho_{\mathrm{n}}}\frac{\partial \rho_{\mathrm{n}}}{\partial r}\right). \tag{12}$$

The decoupling between diffusion and deformation is valid due to the small strain magnitudes. The concentration dependent diffusivity can be defined as $D(\rho_{\mathrm{n}}) = D_0\rho_{\mathrm{m},0}/(\rho_{\mathrm{m},0}-\rho_{\mathrm{n}})$, where $D_0 = Mk_{\mathrm{B}}T$. Eq. 12 can be easily solved numerically, however, we can average the diffusion coefficient (which is similar to one discussed in the Refs.[20,27]):

$$\bar{D} = \frac{1}{\rho_{\mathrm{f}}^{\mathrm{eq}} - \rho_{\mathrm{i}}^{\mathrm{eq}}}\int_{\rho_{\mathrm{i}}^{\mathrm{eq}}}^{\rho_{\mathrm{f}}^{\mathrm{eq}}} D(\rho_{\mathrm{n}})d\rho_{\mathrm{n}} = D_0\frac{\rho_{\mathrm{m},0}}{\rho_{\mathrm{f}}^{\mathrm{eq}} - \rho_{\mathrm{i}}^{\mathrm{eq}}}\ln\left(\frac{\rho_{\mathrm{m},0} - \rho_{\mathrm{i}}^{\mathrm{eq}}}{\rho_{\mathrm{m},0} - \rho_{\mathrm{f}}^{\mathrm{eq}}}\right), \tag{13}$$

where $\rho_{\mathrm{i}}^{\mathrm{eq}}$ and $\rho_{\mathrm{f}}^{\mathrm{eq}}$ are the equilibrium values of intra-particle adsorbate concentrations at the beginning and at the end of a pressure step. Now, using the averaged diffusivity (from Eq. 13) in the Eq. 12 we can write the analytical solutions for the diffusion in spherical geometry.[27] The use of an averaged diffusion coefficient can lead to some deviations from the experimental measurements if the diffusion coefficient changes significantly with concentration. However, the approximation should not change the qualitative description of the kinetic deformation and, if needed, can be overcome using the numerical solution of Eq. 12.

The adsorbate concentration profile and adsorbed amount (N) are given by

$$\frac{\rho_{\mathrm{n}} - \rho_{\mathrm{i}}^{\mathrm{eq}}}{\rho_{\mathrm{f}}^{\mathrm{eq}} - \rho_{\mathrm{i}}^{\mathrm{eq}}} = 1 + \frac{2R}{\pi r}\sum_{\mathrm{n}=1}^{\infty}\frac{(-1)^n}{n}\exp\left\{-\frac{\bar{D}n^2\pi^2 t}{R^2}\right\}\sin\left(\frac{n\pi r}{R}\right) \tag{14}$$

and

$$\frac{N - N_{\mathrm{i}}^{\mathrm{eq}}}{N_{\mathrm{f}}^{\mathrm{eq}} - N_{\mathrm{i}}^{\mathrm{eq}}} = 1 - \frac{6}{\pi^2}\sum_{\mathrm{n}=1}^{\infty}\frac{1}{n^2}\exp\left\{-\frac{\bar{D}n^2\pi^2 t}{R^2}\right\}, \tag{15}$$

respectively.

Summarizing all above written, Eq. 8 and Eq. 9 define the equilibrium adsorbed amount and volumetric deformation, in its turn, Eq. 10, Eq. 14 and Eq. 15 define volumetric de-

formation, adsorbate concentration profile and adsorbed amount during out-of-equilibrium sorption process. In the best case scenario, the model requires adsorption and AID isotherms as well as strain and mass kinetic uptakes to properly quantify the unknown parameters: K, G, $\bar{D}$, λ, κ, $\rho_{m,0}$, b, R.

Results and discussion

We used two sets of experimental data to validate and parametrize the model. Specifically, carbon dioxide adsorption on AC *Chemviron* from Ref.[31] and methane adsorption on *T-3* measured by us. The obtained parameters will be further used to study the possible shapes of kinetic stain curves in microporous materials and to analyze the effect of slow adsorbent deformation on the kinetics of adsorption.

Carbon dioxide on AC Chemviron

Fig.(3) presents the fit of experimental adsorption (a) and strain (b) isotherms taken from Ref.[31] by Eqs. 8 and 9. The calculations were performed for $T = 303$ and 318 K, using the temperature-dependent Langmuir coefficient introduced in the SI. Its value and all additional parameters are summarized in Table 1. We converted the excess adsorption data (both equilibrium and kinetic) to absolute one using the following equation $n_{\text{abs}} = n_{\text{ex}} + v_{\text{micro}}\rho_{\text{b}}$, where $v_{\text{micro}} = 0.51\,\text{cm}^3/\text{g}$ is the microporous volume (taken from Ref.[31]) and ρ_{b} is the carbon dioxide bulk density at the specific temperature and pressure. The temperature-dependent adsorption isotherm fits the experimental data with sufficient accuracy at both temperatures. As was discussed in the Ref.,[31] the experimental data on volumetric strain demonstrate a visible irreversibility, i.e. first adsorption branch is lower than the subsequent cycles (see Fig. 11 from Ref.[31]). We estimated the λ and κ expansion parameters from the fit of experimental data at 303 K. Unfortunately, only two points are available, and it seems that they belong to the first ("irreversible") adsorption branch. Thus, the obtained

values should be taken with reservations. The value for bulk modulus K was taken as 1 GPa, which estimates the magnitude and is supported by the literature values.[14,16] Basically, Eq. 9 contains κ, λ and K as fractions, which complicates their parameterization especially having limited experimental data.

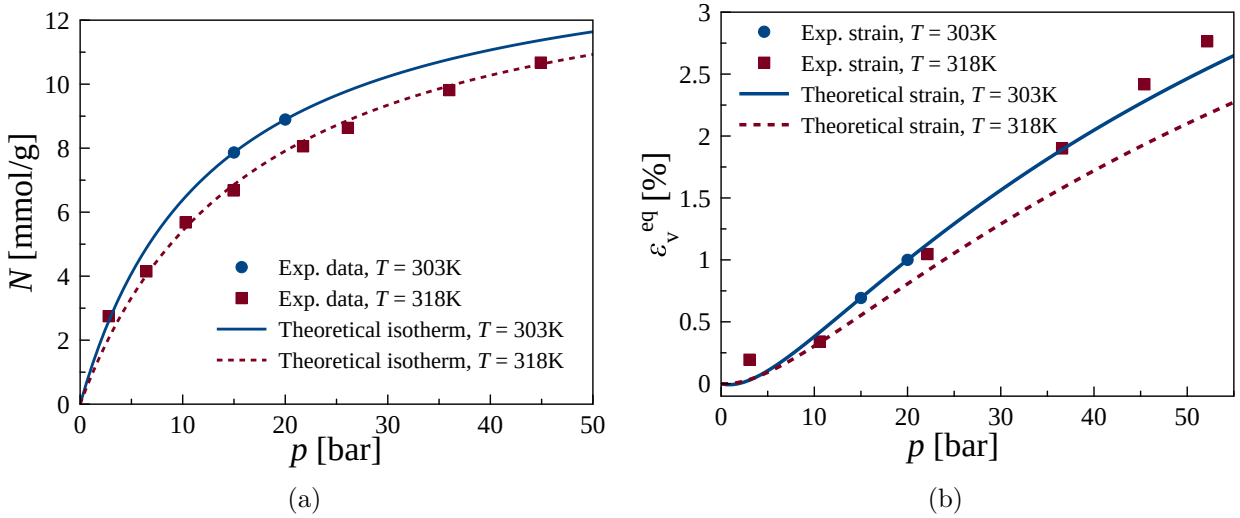

Figure 3: (a) Experimental[31] and theoretical adsorption isotherms at 303 and 318 K. The experimental data corresponds to carbon dioxide adsorption onto AC Chemviron. (b) Experimental[31] and theoretical volumetric strain isotherms at 303 and 318 K. We calculated absolute values of experimental adsorption isotherm as $n_{\text{ex}} + v_{\text{micro}}\rho_{\text{b}}$, where $v_{\text{micro}} = 0.51\,\text{cm}^3/\text{g}$ is the microporous volume (taken from Ref.[31]) and ρ_{b} is the carbon dioxide bulk density at the specific temperature and pressure.

Now, using the obtained values from the Table 1 we can test the model on the experimental data on adsorption and deformation kinetics.[31] The experimental data correspond to two pressure steps: (i) $0 \to 20$ bar and (ii) $20 \to 15$ bar. We combined both of them in Fig. 4, where (a) figure shows the kinetic uptake and (b) - the volumetric strain kinetics. The value of $D_0 = 5 \times 10^{-8}\,\text{m}^2/\text{s}$ was obtained from the (i) pressure step. The corresponding theoretical curves are demonstrated on the Fig. 4 by full lines. The calculations for (ii) step and strain kinetics for (i) step are the predictions as no new parameters were additionally fitted. The mismatch between experiment and theory is the largest in the (ii) case. It can be eliminated by the choice of the D_0 which was demonstrated by the dashed line in Fig. 4. Almost

perfect agreement can be obtained with the kinetic uptake using $D_0 = 1.3 \times 10^{-8}\,\mathrm{m^2/s}$. This discrepancy may be caused by unaccounted processes accompanying the diffusion process, for instance temperature effects during adsorption and desorption process. Also, additional mass transport barrier may contribute to the observed mismatch in diffusivities.

Table 1: Parameters used for comparison with experimental data on AC.[31] The Langmuir parameter (b) is given for 303 K. Additionally, we used the following data from Ref.:[31] specific volume $v_\mathrm{s} = 1.588\,\mathrm{cm^3/g}$. The maximum adsorbed amount is defined as $m = \rho_{0,\mathrm{m}} v_\mathrm{s}$. The radius was calculated from the condition of equal volumes between model particle and the real one, $R = 1.162\,\mathrm{cm}$.

	K [GPa]	b [bar^{-1}]	m [mmol/g]	$\lambda/\rho_{0,\mathrm{m}}$ [-]	ϕ_0/k_B [K]	κ/k_B [K]	D_0[m^2/s]
Adsorption	1	0.0772	14.652	1.669	-1449.5	520	5e-8
Desorption							1.3e-8

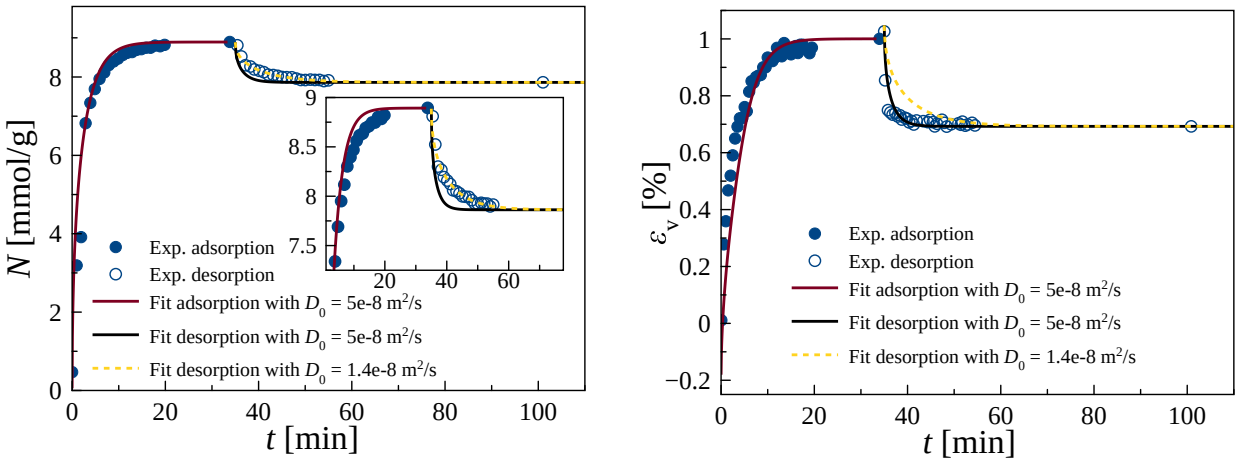

(a) (b)

Figure 4: (a) Experimental[31] and theoretical adsorption uptakes at 303 K for two steps (i) $0 \to 20$ bar and (ii) $20 \to 15$ bar. (b) Experimental[31] and theoretical volumetric strain uptakes at 303 K for two steps (i) $0 \to 20$ bar and (ii) $20 \to 15$ bar. Both experimental and theoretical data from the (ii) step were shifted by 35 min to the right. The experimental data corresponds to carbon dioxide adsorption onto AC Chemviron.

Methane on AC T-3

It is desirable to perform another comparison to better verify the model. Here, we used the data measured by the dilatometric method at fixed pressure and temperature (see experi-

mental section for the measurement details). It allows us to use more conventional method to extract kinetic strain information at the conditions better satisfying modeling assumptions. Additionally, we explored a kinetic behavior of another adsorbate/adsorbent pair – we used methane at 293 K, and the experiment was performed on *T-3* activated carbon. All of that changes helps us to study the model performance independent on experiment technique and adsorbate or adsorbent choice.

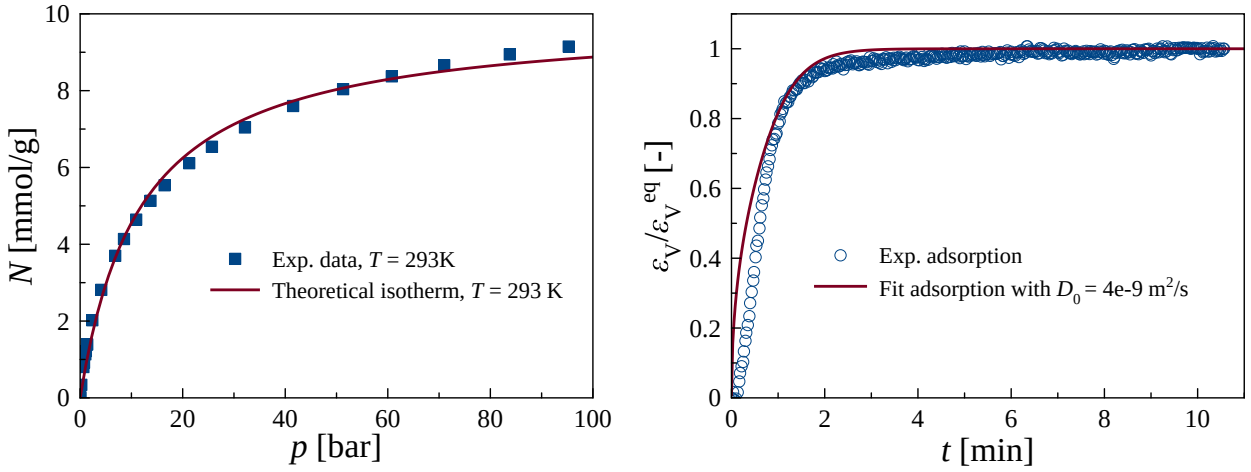

Figure 5: (a) Methane adsorption isotherm on *T-3* measured at 293 K (b) Experimental and theoretical volumetric strain uptakes at 293 K for a pressure step 1 → 99 bar. The strain curves are normalized by the corresponding equilibrium values. The experimental data corresponds to methane adsorption onto AC T-3.

Figs. 5a and 5b show the equilibrium methane adsorption isotherm and normalized kinetic strain uptake, both measured at 293 K. The kinetic uptake was measured for the pressure step 1 → 99 bar and normalized to the equilibrium value. Having only one kinetic curve, we couldn't extract the necessary parameters from the equilibrium strain data. So, we assumed that $\kappa = 0$ and $\lambda k_B T/p \gg 1$. This makes the modeling easier because eliminates the need for the bulk modulus and λ. Note that even under this assumption the volumetric strain still depends on the diffusion process – the normalized strain is a functional of the spatial distribution of the adsorbate inside the material. The corrected diffusivity was obtained from the fit - $D_0 = 4 \times 10^{-9}\,\mathrm{m}^2/\mathrm{s}$. All parameters are summarized in the Table 2.

Table 2: Parameters used for comparison with experimental data on *T-3*. The maximum adsorbed amount is defined as $m = \rho_{0,\mathrm{m}} v_{\mathrm{s}}$. The radius of the spherical particle is equial to 0.171 cm.

	b [bar^{-1}]	m [mmol/g]	ϕ_0/k_{B} [K]	D_0 [m^2/s]
Adsorption	0.085	9.918	-1420	4e-9

General analysis

Up to now, we relied on the experimental data in our analysis. In this section, we consider a hypothetical microporous material. In our calculations we take the same Langmuir parameters as for *Chemviron* AC, thus the adsorption isotherm reproduces the one from Fig. 3 (a). The choice of other parameters is also based on the previously obtained ones (see Table 1).

First of all, the change of the diffusivity leads to the shift of the kinetic volumetric strain curve as it depends on time only through the density profile - Eq. 14. Thus, all the strain curves will be unified if we plot them as a function of $\bar{D}t$ assuming other parameters are equal.

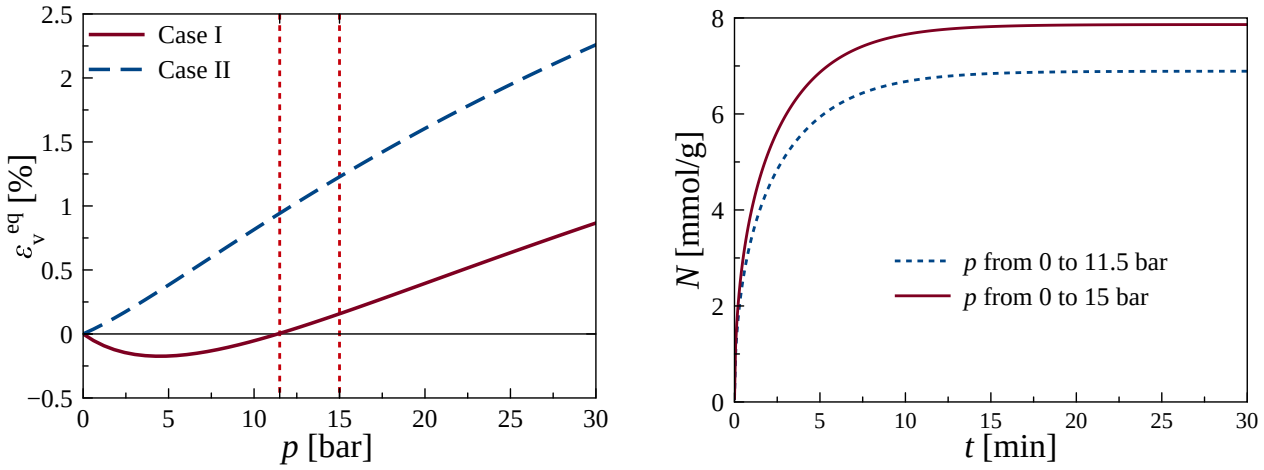

(a) (b)

Figure 6: (a) Theoretical strain isotherms at 303 K and (b) corresponding kinetic uptakes for two pressure steps, i.e. from 0 to 11.5 bar and from 0 to 15 bar. All parameters, except κ, are taken from Table 1 (adsorption). The absolute value of κ was increased by 25% (Case I) ; The value of κ was decreased by 25% (Case II). The curves in (b) corresponds to both cases, while the deformation doesn't affect the diffusion process in the small strain regime.

Several experimental works[1,18,32] demonstrated, that equilibrium adsorption-induced strain as a function of adsorbate bulk pressure can have a minimum. Mostly it is observed in microporous materials, like activated carbons,[18,32] and attributed to the specific combination of adsorbate size and adsorbate-adsorbent interactions. To study this effect better, we calculated the theoretical strain isotherms based on the parameters from Table 1. In order to have two distinct cases we increased (Case I) and decreased (Case II) the value of κ by 25%. The resulting strain isotherms are presented in Fig. 6a. The kinetic adsorption uptakes are shown in Fig. 6b for two different steps: (i) from 0 to 11.5 bar and (ii) from 0 to 20 bar. The first pressure (11.5 bar) is chosen to be near the point of zero volumetric strain for Case I.

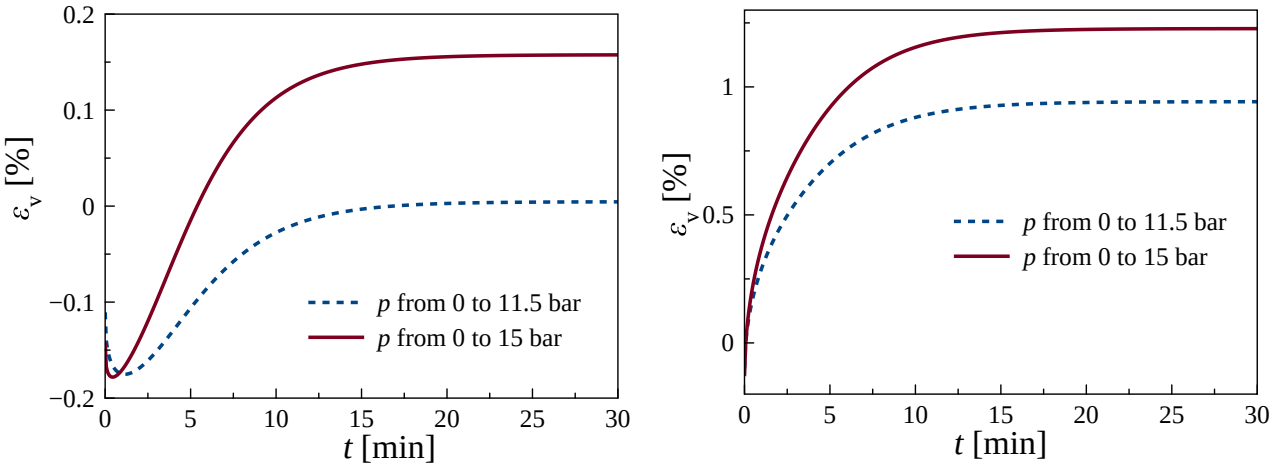

Figure 7: Volumetric strains as a function of time. Calculations were performed for two pressure steps from 0 to 11.5 bar and from 0 to 15 bar. All parameters, except κ, are taken from Table 1 (adsorption). (a) The value of κ was increased by 25% (Case I) and (b) the value of κ was decreased by 25% (Case II) in comparison to the value of the Table 1.

Also, we calculated the kinetic volumetric strains for the same set of parameters and pressure steps, both cases are shown in Figs. 7a and 7b. The calculations for Case II demonstrate similar shapes as were obtained for the adsorption uptakes (see Fig. 6b). However, the curves obtained for Case I have a pronounced minima, as on the equilibrium volumetric strain isotherm. Also, it is interesting, that for the pressure step (i) the sample in the initial and final stages is in the almost undeformed state. However, during the adsorption process,

it goes through the minimum.

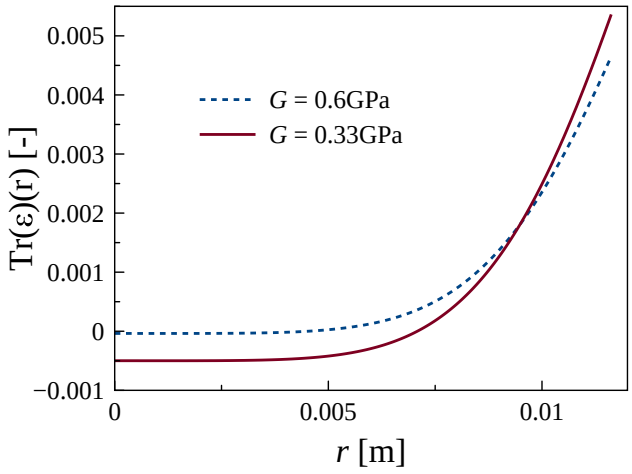

Figure 8: Trace of the strain tensor as a function of distance from the center of particle for two different values of G (the calculations are done at t = 100 s. All other parameters are taken from Table 1 (adsorption).

As was already mentioned, the volumetric deformation is independent of G in our model. However, the local volumetric strain ($Tr(\varepsilon)(r)$) can still be affected. Fig. 8 presents two curves calculated for different values of G, i.e. 0.6 GPa and 0.33 GPa, while all other parameters were taken from Table 1 unaltered. As one can see, a change in shear modulus leads to a redistribution of $Tr(\varepsilon)(r)$ inside the material.

Further discussions

The model is formulated for the ideal case with no variation of pressure in the surrounding reservoir. However, the carbon dioxide kinetic data taken from Ref.[31] were measured using a manometric setup. Unfortunately, the original paper[31] doesn't contain information on the observed pressure drop during adsorbate diffusion. Using the given information we estimated the change in pressure after initial gas expansion (equilibrium pressure in the adsorption step was 20 bar) to be $\approx$ 2 - 3 bar. It justifies the applicability of our model in the description of these data. We don't face the same problem in the case of methane adsorption due to the gas pressure control in the bulk phase during the experiment. Thus, comparisons made

demonstrated that our model can at least qualitatively describe and predict experimental data on kinetic deformation.

Typically, solid bodies deform much faster than the fluid relaxes inside the pores. However, we still can write down the relaxation equation for the hypothetical slow deformation process:

$$\begin{aligned} \frac{\partial u}{\partial t} &= -\Gamma \frac{\delta \Omega}{\delta u} \\ &= \Gamma \left(\left(K + \frac{4}{3} G \right) \frac{\partial}{\partial r} \left[\frac{1}{r^2} \frac{\partial (r^2 u)}{\partial r} \right] + \frac{\partial (f'_{\mathrm{ads}} + p)}{\partial r} \right), \end{aligned} \tag{16}$$

where parameter Γ defines the rate of the deformation, so $\Gamma \ll 1$ is a slow deformation process and $\Gamma \gg 1$ is a fast deformation process. We would like to mention that the first term in the brackets is identical to the one used in the description of gel swelling kinetics.[42,43] This indicates that polymeric materials with a high probability correspond to the slow deformation regime. On the other hand, the typical solid adsorbents, like activated carbon, zeolites, and glasses, should demonstrate fast deformation with $\Gamma \gg 1$. Here, we also need to account for the coupling between diffusion and deformation, because otherwise, the rate of the deformation doesn't affect the adsorption process.

In order to estimate the influence of strain relaxation on adsorption we also used the idea of decoupling adsorption and deformation. Namely, Eq. 16 was solved assuming that the second part on the right-hand side can be estimated using Eq. 14. As a second step, we used the obtained $u(t)$ to numerically calculate the new concentration profile from the diffusion equation (12) with averaged diffusivity $\bar{D}$ and modified boundary condition:

$$\rho_{\mathrm{n}}(R) = \frac{\rho_{\mathrm{m}}(R) b p}{1 + bp}, \tag{17}$$

where ρ_{m}, unlike all other calculations in the paper, depends on $\varepsilon_{\mathrm{V}}(R)$. Thus, as the deformation increases the maximum number of adsorption sites in the material will also increase and the rate of this process could be a limiting one in the slow relaxation case. Using the

parameters from the Table 1 and varying the Γ parameter we calculated adsorption and deformation kinetics for fast and slow relaxations. Figs. 9a and 9b show the time evolution for both cases. The slow relaxation demonstrates the noticeable deviations in both figures. It manifests as a second regime in the Fig. 9a associating with an influence of the deformation process on the adsorption one. As the deformation becomes slow it hinders the adsorption due to the "appearance" of the available adsorption sites in the material. It should be noted that the obtained curve in a slow relaxation regime is similar to the one arising in the non-isothermal model due to the temperature variations.[44] Fig. 9b demonstrates a different behavior of volumetric strains corresponding to fast and slow relaxations at the beginning of the deformation process. In the first case the volumetric strain infinitely fast changes due to the hydrostatic compression. This type of behavior was also observed and reported in Ref.[29,45] However, in the second case, the diffusion rate is fast enough to prevent the contraction by the AID, which leads to the solution without the abrupt decrease.

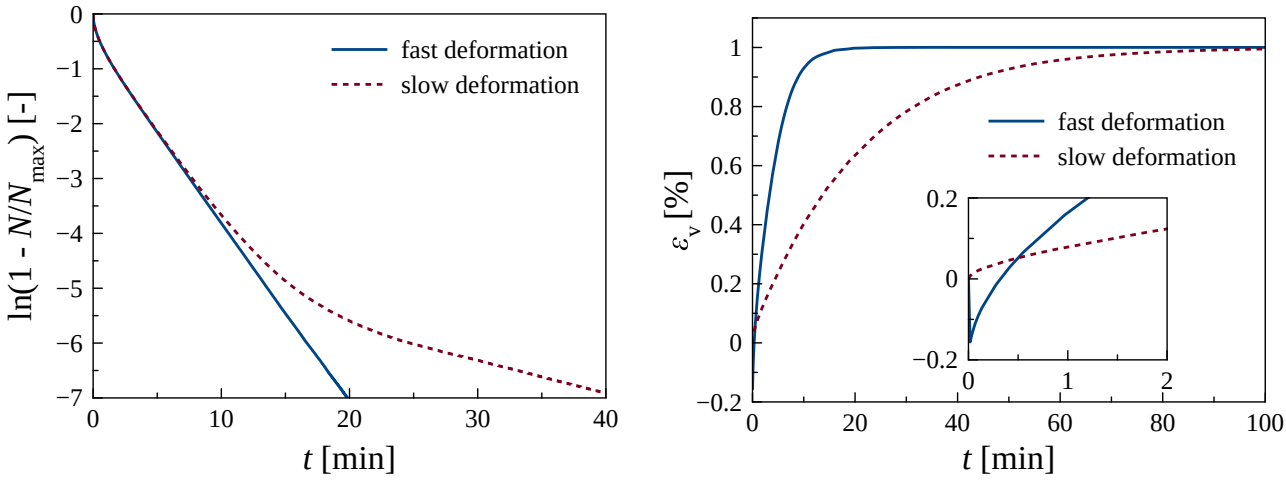

Figure 9: Kinetic uptake (a) and volumetric strains (b) as a function of time. Calculations were performed for a pressure step from 0 to 20 bar. All parameters, are taken from Table 1 (adsorption).

The obtained diffusion parameter ($\bar{D}/R^2$) for both activated carbons covers the following range 10^{-4} – $10^{-3}\,s^{-1}$. It agrees with published values from literature.[46,47] Our values were

extracted independently from the fit of either adsorption or deformation kinetic curves. It suggests, that one can extract the diffusion coefficient directly from the deformation data. However, the lack of experimental data on the well-studied adsorbents doesn't allow us to conclude it with a high degree of confidence.

Another potential application of kinetic AID could be based on its non-invasive measurement possibility (for example, gauge sensor). As the deformation is a non-local quantity, from the surface measurements one can obtain information regarding the sorption, physical or chemical, taking place inside the material. For instance, it may be useful in some industrial applications to study the internal processes in construction. In this case, it can be desirable to maintain the structural integrity during the measurements. Thus, the indirect sorption measurements in place, via AID, could be an alternative to the strategy based on taking samples to the lab.

The previously observed inaccuracies in the simultaneous description of sorption and deformation kinetics of AC *Chemviron* could originate from the model itself. As was mentioned at the beginning of the *Model* section, we used several assumptions and simplifications to formulate the model in an almost fully analytical form. Some of them, for instance, adsorbent geometry and averaged diffusivity, can be easily overcome using numerical methods to solve the differential equations. Others, relating to the properties of the solid material, require significant changes in the model foundations and usage of advanced theoretical techniques. Classical density functional theory, for example, may be used to describe solid-fluid interactions on the scale of one pore so it could improve a description of equilibrium adsorption and strain isotherms. Also, the adsorption process is accompanied by the release or absorption of heat and it should be taken into account as well via additional energy balance equation. We believe, that these modifications could improve the quantitative description of experimental data, but would not change the qualitative conclusions of the paper.

Conclusion

In the work, we studied the kinetics of adsorption-induced deformation of activated carbons using a combination of theoretical and experimental techniques. Our theoretical framework is based on the formulation of the osmotic potential as a functional of two scalar fields - displacement and adsorbate concentration. Minimizing the osmotic potential, we obtained a system of equations describing equilibrium and kinetic sorption and deformation. The out-of-equilibrium sorption process was described using a classical diffusion-based approach providing the time evolution of adsorbate inside the solid material.

Our model was verified by comparison with two sets of experimental data. We demonstrated that the model can describe literature experimental data of carbon dioxide on AC *Chemviron*, namely two sorption curves at 303 K corresponding to pressure steps: (i) $0 \rightarrow 20$ bar and (ii) $20 \rightarrow 15$ bar. Also, we were able to predict volumetric strain kinetic uptake corresponding to the same conditions. Additionally, we measured the deformation kinetics of methane on activated carbon (*T-3*) and applied our model to perform additional verification. We demonstrated that our model is able to describe both experimental sets at least qualitatively with similar accuracy.

Finally, we compared two cases of adsorption-induced deformation, specifically with and without minimum at low bulk adsorbate pressures. Our model predicted that the non-monotonic behavior of equilibrium deformation induces similar patterns in the out-of-equilibrium case. Namely, the theoretical kinetic strain curves also have a minimum at the beginning of the adsorption process. In addition, we predicted the influence of possible host slow relaxations on the kinetic adsorption uptakes. Our calculations suggest that the slow relaxation may hinder the sorption process.

We used several assumptions to reduce the complexity of the final equations, e.g. averaged diffusivity, small strains regime, etc. These approximations and the overall theoretical framework, neglecting a detailed description of inter-atomic interactions, may limit the quantitative predictions of the proposed model. Nevertheless, the current work helps to interpret

experimental data of adsorption-induced deformation, for instance, kinetic curves arising during the equilibration of the sample after step-wise adsorbate pressure increase.

Acknowledgement

AK is grateful to Dr. Jens Möllmer for fruitful discussions. The work was supported by the National Science Foundation, grant CBET-1944495.

Supporting Information Available

Derivation of the main equations for equilibrium and out-of-equilibrium cases.

References

(1) Gor, G. Y.; Huber, P.; Bernstein, N. Adsorption-induced deformation of nanoporous materials—A review. *Appl. Phys. Rev.* **2017**, *4*, 011303.

(2) Kolesnikov, A.; Budkov, Y. A.; Gor, G. Models of adsorption-induced deformation: ordered materials and beyond. *J. Phys. Condens. Matter* **2021**, *34*, 063002.

(3) Vandamme, M. Coupling between adsorption and mechanics (and vice versa). *Curr. Opin. Chem. Eng.* **2019**, *24*, 12–18.

(4) Gor, G. Y.; Scherer, G. W.; Stone, H. A. Bacterial Spores Respond to Humidity Similarly to Hydrogels. *Proceedings of the National Academy of Sciences* **2024**, *121*, e2320763121.

(5) Podbevšek, D.; Jung, Y.; Khan, M.; Yu, H.; Tu, R. S.; Chen, X. The role of water mobility on water-responsive actuation of silk. *Nat. Commun.* **2024**, *15*, 8287.

(6) Hua, L.; Shomali, A.; Zhang, C.; Coasne, B.; Derome, D.; Carmeliet, J. Anisotropic Deformation in a Polymer Slab Subjected to Fluid Adsorption. *Langmuir* **2024**, *40*, 4382–4391.

(7) Masaro, L.; Zhu, X. Physical models of diffusion for polymer solutions, gels and solids. *Progress in polymer science* **1999**, *24*, 731–775.

(8) Yamaue, T.; Doi, M. The stress diffusion coupling in the swelling dynamics of cylindrical gels. *J. Chem. Phys.* **2005**, *122*.

(9) Kolesnikov, A.; Budkov, Y. A.; Basharova, E.; Kiselev, M. Statistical theory of polarizable target compound impregnation into a polymer coil under the influence of an electric field. *Soft Matter* **2017**, *13*, 4363–4369.

(10) Bonavoglia, B.; Storti, G.; Morbidelli, M. Modeling of the sorption and swelling behavior of semicrystalline polymers in supercritical CO2. *Industrial & engineering chemistry research* **2006**, *45*, 1183–1200.

(11) Yang, Y.; Narayanan Nair, A. K.; Sun, S. Sorption and diffusion of methane, carbon dioxide, and their mixture in amorphous polyethylene at high pressures and temperatures. *Industrial & Engineering Chemistry Research* **2021**, *60*, 7729–7738.

(12) Chen, M.; Coasne, B.; Guyer, R.; Derome, D.; Carmeliet, J. Role of hydrogen bonding in hysteresis observed in sorption-induced swelling of soft nanoporous polymers. *Nature communications* **2018**, *9*, 3507.

(13) Chen, M.; Coasne, B.; Derome, D.; Carmeliet, J. Coupling of sorption and deformation in soft nanoporous polymers: Molecular simulation and poromechanics. *Journal of the Mechanics and Physics of Solids* **2020**, *137*, 103830.

(14) Kolesnikov, A. L.; Möllmer, J. Temperature Evolution of Sorbonorit-4 Methane-Induced

Deformation through the Eyes of Classical Density Functional Theory. *Langmuir* **2024**, *40*, 4122–4131.

(15) Emelianova, A.; Balzer, C.; Reichenauer, G.; Gor, G. Y. Adsorption-Induced Deformation of Zeolites 4A and 13X: Experimental and Molecular Simulation Study. *Langmuir* **2023**, *39*, 11388–11397.

(16) Kowalczyk, P.; Furmaniak, S.; Gauden, P. A.; Terzyk, A. P. Carbon dioxide adsorption-induced deformation of microporous carbons. *J. Phys. Chem. C* **2010**, *114*, 5126–5133.

(17) Grégoire, D.; Malheiro, C.; Miqueu, C. Estimation of adsorption-induced pore pressure and confinement in a nanoscopic slit pore by a density functional theory. *Continuum Mech. Therm.* **2018**, *30*, 347–363.

(18) Shkolin, A. V.; Men'shchikov, I. E.; Khozina, E. V.; Yakovlev, V. Y.; Simonov, V. N.; Fomkin, A. A. Deformation of microporous carbon adsorbent sorbonorit-4 during methane adsorption. *J. Chem. Eng. Data* **2022**, *67*, 1699–1714.

(19) Vandamme, M.; Brochard, L.; Lecampion, B.; Coussy, O. Adsorption and strain: the CO2-induced swelling of coal. *J. Mech. Phys. Solids* **2010**, *58*, 1489–1505.

(20) Kärger, J.; Ruthven, D. M.; Theodorou, D. N. *Diffusion in nanoporous materials*; Wiley Online Library, 2012; Vol. 48.

(21) Sircar, S.; Hufton, J. Why does the linear driving force model for adsorption kinetics work? *Adsorption* **2000**, *6*, 137–147.

(22) Son, F. A.; Shi, K.; Snurr, R. Q.; Farha, O. K. Measuring Mass Transfer of n-Hexane and 2-Chloroethyl Ethyl Sulfide in Sorbent/Polymer Fiber Composites Using a Volumetric Adsorption Apparatus. *ACS Appl. Mater. Interfaces* **2024**, *16*, 31534–31542.

(23) Preißler-Kurzhöfer, H.; Kolesnikov, A.; Lange, M.; Möllmer, J.; Erhart, O.; Kobalz, M.;

Hwang, S.; Chmelik, C.; Krautscheid, H.; Gläser, R. Hydrocarbon sorption in flexible MOFs—Part II: understanding adsorption kinetics. *Nanomaterials* **2023**, *13*, 601.

(24) Neimark, A. V.; Coudert, F.-X.; Boutin, A.; Fuchs, A. H. Stress-based model for the breathing of metal- organic frameworks. *J. Phys. Chem. Lett.* **2010**, *1*, 445–449.

(25) Coudert, F.-X.; Jeffroy, M.; Fuchs, A. H.; Boutin, A.; Mellot-Draznieks, C. Thermodynamics of guest-induced structural transitions in hybrid organic- inorganic frameworks. *J. Am. Chem. Soc.* **2008**, *130*, 14294–14302.

(26) Bousquet, D.; Coudert, F.-X.; Fossati, A. G.; Neimark, A. V.; Fuchs, A. H.; Boutin, A. Adsorption induced transitions in soft porous crystals: An osmotic potential approach to multistability and intermediate structures. *J. Chem. Phys.* **2013**, *138*.

(27) Crank, J. *The mathematics of diffusion*; Oxford university press, 1979.

(28) Pini, R.; Ottiger, S.; Burlini, L.; Storti, G.; Mazzotti, M. Role of adsorption and swelling on the dynamics of gas injection in coal. *J. Geophys. Res.: Solid Earth* **2009**, *114*, B04203.

(29) Sampath, K.; Perera, M.; Matthai, S.; Ranjith, P.; Dong-yin, L. Modelling of fully-coupled CO2 diffusion and adsorption-induced coal matrix swelling. *Fuel* **2020**, *262*, 116486.

(30) Wang, K.; Wang, Y.; Guo, H.; Zhang, J.; Zhang, G. Modelling of multiple gas transport mechanisms through coal particle considering thermal effects. *Fuel* **2021**, *295*, 120587.

(31) Perrier, L.; Plantier, F.; Grégoire, D. A novel experimental setup for simultaneous adsorption and induced deformation measurements in microporous materials. *Rev. Sci. Instrum.* **2017**, *88*, 035104.

(32) Kowalczyk, P.; Ciach, A.; Neimark, A. V. Adsorption-induced deformation of microporous carbons: Pore size distribution effect. *Langmuir* **2008**, *24*, 6603–6608.

(33) Men'shchikov, I.; Shiryaev, A.; Shkolin, A.; Vysotskii, V.; Khozina, E.; Fomkin, A. Carbon adsorbents for methane storage: genesis, synthesis, porosity, adsorption. *Korean J. Chem. Eng.* **2021**, *38*, 276–291.

(34) *Neopredelennost' Izmereniya, Chast' 3, Rukovodstvo po vyrazheniyu neopredelennosti izmereniya (ISO/IEC Guide 98-3:2008, IDT)*; Standartinform, 2018.

(35) Shkolin, A.; Men'shchikov, I.; Fomkin, A. Method to measure the deformation of nanoporous materials induced by the adsorption of gases and vapors. *Nanobiotechnology Reports* **2022**, *17*, 925–931.

(36) Shkolin, A.; Men'shchikov, I.; Khozina, E.; Yakovlev, V. Y.; Fomkin, A. Isotropic and anisotropic properties of adsorption-induced deformation of porous carbon materials. *Adsorption* **2023**, *29*, 237–253.

(37) Ravikovitch, P. I.; Neimark, A. V. Density functional theory model of adsorption deformation. *Langmuir* **2006**, *22*, 10864–10868.

(38) Pulin, A.; Fomkin, A.; Sinitsyn, V.; Pribylov, A. Adsorption and adsorption-induced deformation of NaX zeolite under high pressures of carbon dioxide. *Russ. Chem. Bull., Int. Ed.* **2001**, *50*, 60–62.

(39) Amberg, C.; McIntosh, R. A study of adsorption hysteresis by means of length changes of a rod of porous glass. *Can. J. Chemistry* **1952**, *30*, 1012–1032.

(40) Landau, L. D.; Lifshitz, E. M.; Kosevich, A. M.; Pitaevskii, L. P. *Theory of elasticity: volume 7*; Elsevier, 1986; Vol. 7.

(41) Hughes, A. P.; Thiele, U.; Archer, A. J. An introduction to inhomogeneous liquids, density functional theory, and the wetting transition. *Am. J. Phys.* **2014**, *82*, 1119–1129.

(42) Wahrmund, J.; Kim, J.-W.; Chu, L.-Y.; Wang, C.; Li, Y.; Fernandez-Nieves, A.; Weitz, D. A.; Krokhin, A.; Hu, Z. Swelling kinetics of a microgel shell. *Macromolecules* **2009**, *42*, 9357–9365.

(43) Tanaka, T.; Fillmore, D. J. Kinetics of swelling of gels. *J. Chem. Phys.* **1979**, *70*, 1214–1218.

(44) Sircar, S. Linear-driving-force model for non-isothermal gas adsorption kinetics. *J. Chem. Soc., Faraday Trans. 1 F* **1983**, *79*, 785–796.

(45) Zhao, W.; Wang, K.; Liu, S.; Ju, Y.; Zhou, H.; Fan, L.; Yang, Y.; Cheng, Y.; Zhang, X. Asynchronous difference in dynamic characteristics of adsorption swelling and mechanical compression of coal: Modeling and experiments. *Int. J. Rock Mech. Min.* **2020**, *135*, 104498.

(46) Magalhães Siqueira, R.; Vilarrasa-García, E.; Belo Torres, A. E.; Silva de Azevedo, D. C.; Bastos-Neto, M. Simple procedure to estimate mass transfer coefficients from uptake curves on activated carbons. *Chem. Eng. Technol.* **2018**, *41*, 1622–1630.

(47) Ju, Y.; Park, Y.; Park, D.; Kim, J.-J.; Lee, C.-H. Adsorption kinetics of CO_2, CO, N_2 and CH_4 on zeolite LiX pellet and activated carbon granule. *Adsorption* **2015**, *21*, 419–432.

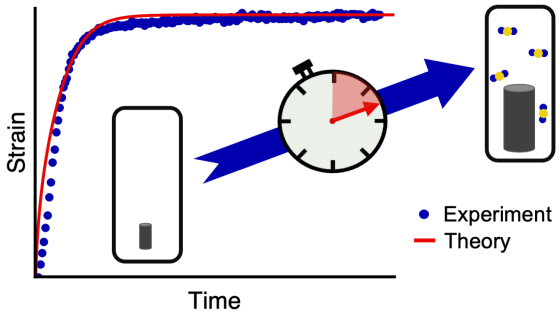

For Table of Contents Only